Indian Journal of Chemistry
Vol. 31A, August 1992, pp. 483-491

Nonlinear dynamics in proton-noble gas atom collisions†

B M Deb

Theoretical Chemistry Group, Department of Chemistry, Panjab University, Chandigarh 160 014

Some recent works from our laboratory on time-dependent (TD) quantum-fluid density-functional studies of high-energy (25 keV) proton-neon and proton-helium atom collisions have been reviewed. These result: in two generalized non-linear Schrödinger equations (GNLSE), depending on the forms of the various density functionals employed. The numerical solutions of these equations yield various time-dependent quantities in three-dimensional space, e.g., electronic charge density, current density, difference density, effective potential surface as well as TD induced dipole moment, dipole polarizability, etc. The approach enables one to follow a collision process from start to finish, in course of time, thereby providing fresh insights into the mechanism of a collision process and identifying the non-linear features, if any, of the process which permits excitation but not ionization. One of the most interesting observations in this study is a natural partitioning of the collision process into *approach*, *encounter* and *departure* regimes. Our approach has involved a simultaneous consideration of three crucial problems in density-functional theory, namely, time-dependence, excited states and a satisfactory kinetic energy-density functional. Further, the phase associated with the hydrodynamic "wave function" has been related to Berry's geometrical phase in quantum mechanics.

In recent years, there have emerged two major areas of development in the quantum theories of many-electron systems, which depend on the single-particle density[1] as the basic variable, instead of the many-electron wave function. These are: density functional theory (DFT)[1-4] and quantum fluid dynamics (QFD)[5-7]. This article describes a synthesis of these two approaches to deal with time-dependent non-reactive collisions between a proton and a noble gas atom, e.g., He or Ne.

In spite of its remarkable successes in explaining the electronic structure, binding and other properties of atoms, molecules and solids, DFT has mainly been restricted to the ground state and to time-independent situations. In other words, atomic and molecular collilsions were not dealt with by general DFT, although some efforts were earlier made[8,9] in the context of the Thomas-Fermi theory[12]. On the other hand, it has been clear for some time[5-7] that if one could bring about a merging together of DFT and QFD, viz. the "classical" hydrodynamical analogy to quantum mechanics, then this would form an interesting theory of many-electron systems, for both time-independent and time-dependent situations, in which the many-particle wave function is replaced by the single-particle charge density and current density. This approach would have the simplicity of treating time-dependent (TD) processes in terms of a single, one-particle TD equation of motion (EOM). Since it involves the hydrodynamical analogy, it lends additional support to the continuing efforts[7] to obtain "classical" interpretations of quantum mechanics and also paves the way to a formal "thermodynamic" description of an individual many-electron system.

An attempt to deal with the mechanism of a TD atomic or molecular scattering process in terms of the single-particle densities, would essentially involve the time-evolution of the electronic charge density, current density, a pulsating effective potential surface and other TD quantities which would help in monitoring the process from start to finish. Clearly, this is a different approach from that usually resorted to in molecular dynamics. However, this approach is confronted with three formidable problems in modern DFT: (a) time-dependence, (b) excited states and (c) a satisfactory kinetic energy density (KED) with proper local and global behaviour as well as a proper functional derivative. As we shall see below, the QFDFT approach described in this article involves a combined attack on all these three problems.

In the next section, we summarize the basic principles of DFT and QFD for many-electron systems in three-dimensional space. The subsequent section deals with the QFDFT approach for proton-neon

†Presented at the All India Symposium on "Structure, Activity and Dynamics—Advancing Frontiers" held on the occasion of 65th birthday of Prof. R.P. Rastogi.

collisions while the next section discusses proton-helium collisions. We then comment briefly on the relation between Berry's geometrical phase[10] in quantum mechanics and the phase of the electronic hydrodynamical function[6,7] in QFD. Finally, the last section offers a few concluding remarks.

Basic principles of DFT and QFD for many-electron systems in three-dimensional space

Summary of DFT

In 1964, Hohenberg and Kohn[11] had proved two theorems which provided the quantum-mechanical justification for considering the electron density $\rho(\mathbf{r})$ as a fundamental variable. Their first theorem proved that the non-degenerate ground state of N particles moving under the influence of their mutual coulomb repulsion and a static external single-particle potential $v(\mathbf{r})$ arising, e.g. from a set of nuclei embedded in an electron gas, is completely characterized by $\rho(\mathbf{r})$. In other words, $v(\mathbf{r})$, ψ and hence all ground-state properties of the system are unique functionals of the electron density.

The second theorem of Hohenberg and Kohn proved that, for a given external potential, the energy functional $E[\rho]$ assumes a minimum value for the true density.

Thus, both the ground-state density ρ and energy E can be variationally determined by minimizing the energy functional $E[\rho]$ with respect to the trial density, subject to the normalization constraint (atomic units employed throughout this paper, except the following subsection),

$$\int \rho(\mathbf{r})d\mathbf{r} = N \qquad \ldots(1)$$

One therefore uses the stationary condition.

$$\delta\{E[\rho] - \mu \int \rho(\mathbf{r})d\mathbf{r}\} = 0 \qquad \ldots(2)$$

to obtain the Euler-Lagrange equation

$$\frac{\delta E}{\delta \rho} = \mu \qquad \ldots(3)$$

where μ is a Lagrange multiplier (chemical potential). This has been identified as $(\partial E/\partial N)$ which is the negative of electronegativity[12].

Kohn and Sham[13] had derived a set of single-particle equations by mapping the system of N interacting electrons on to a system of N non-interacting fermions or quasi-particles where every particle moves in an "average" field due to the nuclei and other electrons. The set of equations are,

$$v_{eff}(\mathbf{r},\rho) + \frac{\delta T}{\delta \rho} = \mu \qquad \ldots(4)$$

$$v_{eff}(\mathbf{r},\rho) = v(\mathbf{r}) + \int \frac{\rho(\mathbf{r}')}{|\mathbf{r}-\mathbf{r}'|} d\mathbf{r}' + \frac{\delta E_{xc}}{\delta \rho} \qquad \ldots(5)$$

$$\left[-\frac{1}{2}\nabla^2 + v_{eff}(\mathbf{r},\rho)\right]\phi_i = \varepsilon_i \phi_i ; i = 1, \ldots, N \qquad \ldots(6)$$

$$\rho(\mathbf{r}) = \sum_{\text{lowest } N_{\text{normalized}} \phi i} |\phi_i(\mathbf{r})|^2 \qquad \ldots(7)$$

$$E = \sum_i \varepsilon_i - \frac{1}{2}\iint \frac{\rho(\mathbf{r})\rho(\mathbf{r}')}{|\mathbf{r}-\mathbf{r}'|} d\mathbf{r}d\mathbf{r}' + E_{xc} - \int \rho(\mathbf{r}) \frac{\delta E_{xc}}{\delta \rho} d\mathbf{r} \qquad \ldots(8)$$

$$T = \sum_i \varepsilon_i - \int \rho(\mathbf{r}) v_{eff}(\mathbf{r},\rho) d\mathbf{r} \qquad \ldots(9)$$

For the significance of various terms in Eqs. (4)-(9), the reader may consult ref. 2. E, T and E_{xc} are the total electronic, kinetic and exchange-correlation energies respectively; $v_{eff}(\mathbf{r}, \rho)$ is an effective potential occurring in the set of N non-linear single-particle Eq. (6). The Kohn-Sham equations retain the particle (orbital) picture for the system and exactly treat the kinetic energy . Note that here N equations are to be solved self-consistently and the eigenvalues $\{\varepsilon_i\}$ do not obey Koopmans theorem. For details of DFT, the reader may consult refs. 1-6.

Summary of QFD

In 1926, Madelung[14] transformed the Schrödinger equation for a particle into two fluid-dynamical equations with classical appearance, viz. a continuity equation and an Euler-type EOM. This description involved the density $\rho(=|\psi|^2)$ and the velocity field $\mathbf{v}$ as the primary quantities. Interestingly, the continuous nature of the density gives this quantum fluid more fluid-like character than a classical fluid! This indicates the possibility of a "classical" description of quantum systems through the fluid-dynamical viewpoint.

For a single-particle system, if one writes the wave function ψ in the polar form (atomic units not employed in this sub-section for the sake of clarity),

$$\psi(\mathbf{r},t) = R(\mathbf{r},t)\exp[iS(\mathbf{r},t)/\hbar] \qquad \ldots(10)$$

then the TD Schrödinger equation,

$$-\frac{\hbar^2}{2m}\nabla^2\psi + V\psi = i\hbar\frac{\partial \psi}{\partial t} \qquad \ldots(11)$$

is transformed into two QFD equations, as mentioned above, viz.

$$\text{Continuity equation: } \frac{\partial \rho}{\partial t} + \nabla.(\rho \mathbf{v}) = 0 \qquad \ldots(12)$$

$$\text{Equation of motion: } m\rho \frac{\delta \mathbf{v}}{dt} = -\rho \nabla (V + V_{qu}) \qquad \ldots(13)$$

$$= \text{Net local force density,}$$

where

$$\frac{d\mathbf{v}}{dt} = \frac{\partial \mathbf{v}}{\partial t} + (\mathbf{v}.\nabla)\mathbf{v} \qquad \ldots(14)$$

$$S = R^2 \qquad \ldots(15)$$

$$\mathbf{v} = \frac{1}{m} \nabla S, \text{ irrotational when } \psi \neq 0 \qquad \ldots(16)$$

V_{qu} = Quantum (Bohm) potential arising from kinetic energy

$$= -\frac{\hbar^2}{2m} \frac{\nabla^2 R}{R}$$

V = Coulomb potential.

In this hydrodynamical analogy to the quantum mechanics of a single-particle system, the time-evolution of the system is interpreted in terms of a flowing fluid of density $\rho(\mathbf{r}, t)$ and a velocity field $\mathbf{v}(\mathbf{r}, t)$, subjected to forces arising from V and V_{qu}, i.e. both classical and quantum forces. Thus, in this picture ψ is replaced by ρ and $\mathbf{v}$ while the particle is replaced by a continuous fluid.

One can also write the following "classical" relations:

$$\mathbf{u} = -\frac{i\hbar}{m} \frac{\nabla \psi}{\psi} = \mathbf{v} + i\mathbf{v}_i; \mathbf{v}_i = -\frac{\hbar}{2m} \nabla \ln \rho;$$

$$\nabla \times \mathbf{v}_i = 0 \text{ when } \rho \neq 0 \qquad \ldots(18)$$

$$\int \rho \nabla \overline{V_{qu} d\mathbf{r}} = 0 \qquad \ldots(19)$$

$$m \frac{d}{dt} \langle \mathbf{v} \rangle = -\langle \nabla V \rangle; \langle \mathbf{v} \rangle = \frac{d}{dt} \langle \mathbf{r} \rangle \qquad \ldots(20)$$

$$\langle \mathbf{r} \times \nabla V_{qu} \rangle = 0 \qquad \ldots(21)$$

The stationary states of the system may be classified as,

(i) Static, with $\mathbf{v} = 0$ and $\nabla(V + V_{qu}) = 0$, indicating the balance between classical and quantum forces, e.g., the $1s$ state of the H atom.

(ii) Dynamics, with $\mathbf{v} \neq 0$ and $\nabla(V + V_{qu}) \neq 0$, so that there is no balance between classical and quantum forces and the fluid has a kinetic energy of $\frac{1}{2}mv^2$. Examples are $2p_1$ and $2p_{-1}$ states of the H atom.

Furthermore, when $\Psi = 0$ (node), S and ∇S are not well defined. Hence, the vorticity, defined as

$$\boldsymbol{\omega} = \nabla \times \mathbf{v} \qquad \ldots(22)$$

does not vanish at the nodal points, causing the so-called "quantum whirlpools". Hirschfelder *et al.*[15] have depicted and discussed the streamlines and vorticities of the electron fluid in an atom or molecule.

However, for an N-electron system, Madelung fluid dynamics in 3N-dimensional configuration space are merely of mathematical curiosity, with very little interpretive potential. Therefore, the QFD equations for a many-electron system should be brought to three-dimensional space so that the fluid-dynamical description could be in terms of the electron density $\rho(\mathbf{r})$ and the current density $\mathbf{j}(\mathbf{r})$ both of which are local observables because they can be related to local Hermitian operators (note that the velocity field $\mathbf{v}(\mathbf{r})$ is not a local observable).

This projection of N-particle QFD equations onto the three-dimensional space can be done in terms of an orbital partitioning of $\rho(\mathbf{r})$ and $\mathbf{j}(\mathbf{r})$, e.g., in terms of natural orbitals[16] or Kohn-Sham orbitals $\{\phi_i\}$[17], with occupation nubers $\{\eta_i\}$. Then,

$$\rho(\mathbf{r}) = \sum_i \eta_i \rho_i; \rho_i = |\phi_i|^2 \qquad \ldots(23)$$

$$\mathbf{j}(\mathbf{r}) = \sum_i \eta_i \mathbf{j}_i; \mathbf{j}_i = \frac{1}{m} \rho_i \nabla S_i \qquad \ldots(24)$$

$$\phi_i = R_i \exp[iS_i/\hbar] \qquad \ldots(25)$$

and one has a continuity equation as well as an Euler-type equation of motion for every orbital. For both these equations, summation over occupied orbitals can be performed to give the continuity equation and the EOM involving the net $\rho(\mathbf{r})$ and $\mathbf{j}(\mathbf{r})$. Here, each individual velocity field $\mathbf{v}^i$ is irrotational but the net velocity field $\mathbf{v}$ is rotational. It has also been shown by us that since $\rho(\mathbf{r})$ and $\mathbf{j}(\mathbf{r})$ are both hydrodynamical quantities, there is an intimate relationship between DFT and QFD. Such relationship provides the foundations on which TDDFT rests[18]. TDDFT had led to the earliest calculation of frequency-dependent multipole polarizabilities (linear response) of, e.g., noble gas atoms[19]. For more details of the QFD approach, the reader may consult refs. 5-7.

A quantum-fluid density-functional theory (QFDFT) of high-energy proton-neon collisions

This section is based mainly on ref. 20. The formal existence[18] of a TDDFT enables one to write the QFD equations in three-dimensional space in terms of TD charge density $\rho(\mathbf{r}, t)$ and the velocity potential (or the phase function) $x(\mathbf{r}, t)$ as (atomic units employed),

$$\frac{\partial \rho}{\partial t} + \nabla . (\rho \nabla x) = 0 \quad \ldots(26)$$

$$\frac{\partial x}{\partial t} + \frac{1}{2}(\nabla x)^2 + \frac{\delta G[\rho]}{\delta \rho} + \int \frac{\rho(\mathbf{r}', t)}{|\mathbf{r} - \mathbf{r}'|} d\mathbf{r}' + v(\mathbf{r}, t) = 0 \quad \ldots(27)$$

$$\phi(\mathbf{r}, t) = \rho^{1/2}(\mathbf{r}, t) \exp[ix(\mathbf{r}, t)]; \rho = |\phi|^2 \quad \ldots(28)$$

$$G[\rho] = T[\rho] + E_{xc}[\rho] \quad \ldots(29)$$

$$E_x[\rho] = -C_x \int \rho^{4/3}(\mathbf{r}) d\mathbf{r}; C_x = (3/4\pi)(3\pi^2)^{1/3} \quad \ldots(30)$$

For studying proton-neon collisions[20], the correlation energy functional $E_c[\rho]$ has been neglected. However, a local correlation functional would be employed for proton-helium collilsions[21], in the next section. The phase function $x(\mathbf{r}, t)$ is space-independent for the stationary ground state of a system whereas for excited and TD states, $x(\mathbf{r}, t)$ has been related[22] to an internal magnetic field and Berry's geometrical phase[10]. The external TD potential $v(\mathbf{r}, t)$ which is a unique functional of $\rho(\mathbf{r}, t)$ can be written for the *p*-Ne scattering system as,

$$v(\mathbf{r}, t) \equiv v(\mathbf{r}, \mathbf{R}, t) = -\left[\frac{Z}{r} + \frac{1}{|\mathbf{R}(t) - \mathbf{r}|}\right] \quad \ldots(31)$$

where Z is the nuclear charge of the Ne atom and $|\mathbf{R}|$ is the internuclear distance. For the given problem, the KE functional is taken as

$$T[\rho] = \int \{t_{at}[\rho] + t_{mol}[\rho]\} d\mathbf{r} \quad \ldots(32)$$

where

$$t_{at}[\rho] = C_K \rho^{5/3} + \frac{1}{8}\frac{(\nabla\rho)^2}{\rho} + a(N)\left[\frac{\mathbf{r}.\nabla\rho}{r^2} - \frac{1}{2}\nabla^2\rho\right] \quad \ldots(33)$$

$$t_{mol}[\rho] = \frac{f(R, N)}{N}\rho \quad \ldots(34)$$

$$f(R, N) = 1/R^{12} - (N/10)^{14} R^2 \exp(-0.8R) \quad \ldots(35)$$

with $C_K = (3/10)(3\pi^2)^{2/3}$; a(N) is taken from Ghosh and Balbas[23], f(R, N) is the change in electronic kinetic energy,

$$\Delta T(R) = T(R) - T(\infty) = \int t_{mol}[\rho] d\mathbf{r} = f(R, N),$$

on molecule formation. Figure 1 depicts this change for a diatomic molecule containing ten electrons.

Now, if one eliminates the velocity potential x between the two QFD Eqs (26) and (27), one obtains a generalized non-linear Schrödinger equation (GNLSE) which describes the dynamics of the *p*-Ne colliding system

$$\left[-\frac{1}{2}\nabla^2 + v_{eff}(\mathbf{r}, t)\right]\phi(\mathbf{r}, t) = i\frac{\partial \phi(\mathbf{r}, t)}{\partial t} \quad \ldots(36)$$

where $v_{eff}(\mathbf{r}, t)$ is a pulsating (TD) potential surface on which the process occurs and is given by

$$v_{eff}(\mathbf{r}, t) = \frac{5}{3}C_K\rho^{2/3} - \frac{4}{3}C_x\rho^{1/3} - \frac{a(N)}{r^2} - U(\mathbf{r}) - \frac{1}{|\mathbf{R} - \mathbf{r}|} + \frac{f(R, N)}{N} \quad \ldots(37)$$

In Eq. (37), $U(\mathbf{r})$ is the electrostatic potential[24].

$$U(\mathbf{r}) = \frac{Z}{r} - \int \frac{\rho(\mathbf{r}', t)}{|\mathbf{r} - \mathbf{r}'|} d\mathbf{r}' \quad \ldots(38)$$

At this stage, it is necessary to make the following observations regarding the above approach:

1. $\phi(\mathbf{r}, t)$ is a TD single "orbital" for the entire many-electron system.

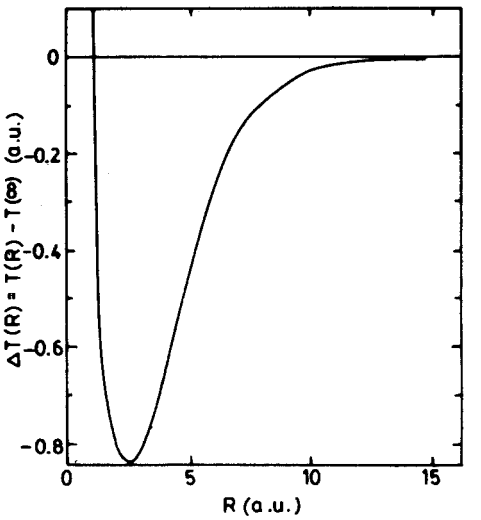

Fig. 1—Change in electronic kinetic energy on molecule formation, as a function of the internuclear distance, for a diatomic molecule containing ten electrons (reproduced from ref. 20; courtesy, American Physical Society).

2. Eq. (36) may be formally regarded as describing the dynamics of a "non-interacting" system of particles where the KE part is represented by the Laplacian operator and all relevant interactions are incorporated in v_{eff}.

3. The non-linearity in the GNLSE, Eq. (36), arises from both non-integer powers of ρ and the integral in $U(\mathbf{r})$.

4. $\phi(\mathbf{r}, t)$ does not obey a linear superposition principle. Its amplitude yields the charge density $\rho(\mathbf{r}, t)$ and its phase yields the current density $\mathbf{j}(\mathbf{r}, t) = \rho \nabla x = [\phi_{re} \nabla \phi_{im} - \phi_{im} \nabla \phi_{re}]$.

5. The dynamics of the system/process can be studied in terms of $\rho(\mathbf{r}, t)$, $\mathbf{j}(\mathbf{r}, t)$ and $v_{eff}(\mathbf{r}, t)$, etc. or any suitable partitioning of them.

(i) $\rho(\mathbf{r}, t)$ describes the dynamics of charge reorganization in the system due to perturbation, e.g., the flow of charge from one region to another, collective density oscillations, etc.

(ii) AT $t = 0$, when the system is in its ground state, $\mathbf{j}(\mathbf{r}, t)$ vanishes. As the interaction progresses with time, $\mathbf{j}(\mathbf{r}, t)$ will be non-vanishing due to the mixing of the excited states with the ground state, under the perturbation. The quantity $\mathbf{j}(\mathbf{r}, t)$ can convey information about streamlines, vorticities, magnetic effects, etc. generated by a given perturbation.

6. In the present collision process, excitation is permitted but ionization is not, and

$$v_{eff}(\mathbf{r}, t) \to 0 \text{ as } r \to \infty, \forall t,$$

7. Eq. (36) may be more advantageous compared to TDKS, TDHF and TDTF approaches, all of whom require the solution of more than one equation for many-electron systems.

8. The coupling between electronic KE and interelectronic repulsion energy has not been considered.

9. When the time-evolving dispersive (due to the Laplacian) and non-linear terms balance each other, solitions or solitary waves may be generated.

As mentioned above, through Eq. (36), one may consider the N-electron molecular system as an ideal system of N non-interacting particles moving under the potential $v_{eff}(\mathbf{r}, t)$ and by analogy, bring in the required classical relations for an ideal monoatomic gas by replacing the average number density N/V locally by $\rho(\mathbf{r}, t)$. One may then look at the dynamics of the system in terms of a space-time-dependent internal "temperature", entropy density and chemical potential for the entire time-evolving system. The quantity $\mu(\mathbf{r}, t)$ should describe the dynamical evolution of the system from $\mu_{initial}$ to μ_{final}, both being constant over whole space, according to ground-state DFT. Thus, it is possible to obtain the following and other "thermodynamic" relations[20] for the molecular electron gas in an internally consistent manner, in terms of ρ, $\mathbf{j}$, v_{eff}, μ and Θ (atomic units employed)

$$\text{KED: } t(\mathbf{r}, \rho) = \frac{3}{2} \rho k \Theta + \frac{1}{2\rho} |\mathbf{j}|^2, \qquad \ldots(39)$$

where Θ is an "internal temperature", and k is the Boltzmann constant (a.u.)

$$\text{Entropy density: } S(\mathbf{r}, t) = \frac{3}{2} k\rho \ln \Theta - k\rho \ln \rho + \frac{1}{2} k\rho \left[5 + 3 \ln (k/2\pi)\right] \qquad \ldots(40)$$

$$\text{Chemical potential: } \mu(\mathbf{r}, t) = v_{eff} + k\Theta \ln \rho - \frac{3}{2} k\Theta \ln (k\Theta/2\pi) \qquad \ldots(41)$$

Once ρ, $\mathbf{j}$ and v_{eff} are calculated by solving Eq. (36), the above quantities can also be obtained.

Another point of interest to note is that there is a correspondence between the single-particle QFDFT Eq. (36), dealing with the motion of a generalized Madelung fluid and the classical dynamics of a particle of mass m undergoing diffusion in a medium, with diffusion coefficient v, according to a Markov process. Taking $\vartheta = \hbar/2m$, it is possible to derive[20] Eq. (36) according to Nelson's stochastic mechanics[25].

Equation (36) has been solved numerically (see ref. 20 for details) for 25 keV p-Ne head-on collisions, in cylindrical polar coordinates. Some of the results are depicted in Fig. 2 for $v_{eff}(\mathbf{r}, t)$, $\rho(\mathbf{r}, t)$ and $|\mathbf{j}(\mathbf{r}, t)|$ at $t = 0.08$ and $R = 9.92$ a.u. The oscillations of the entire potential surface $v_{eff}(\mathbf{r}, t)$ manifest themselves clearly [Fig. 2(a)]. The peaks (repulsive) and troughs (attractive) occur due to the relative magnitudes of the attractive and repulsive terms in v_{eff}, Eq. (37). Although the entire collision process was visualized in terms of three regimes, viz. *approach*, *encounter* and *departure*, only the $0 \leqslant t \leqslant 0.08$ and $9.92 \leqslant R \leqslant 10$ ranges (approach regime) could be covered in these calculations, due to limitations on computational resources. Both ρ and $|\mathbf{j}|$ show prominent collective oscillations, particularly in their outer regions, along the $\hat{z}$ direction. The attractive zones in v_{eff} tend to cause an accumulation of electronic charge in these zones while the repulsive zones tend to cause a depletion of electronic charge.

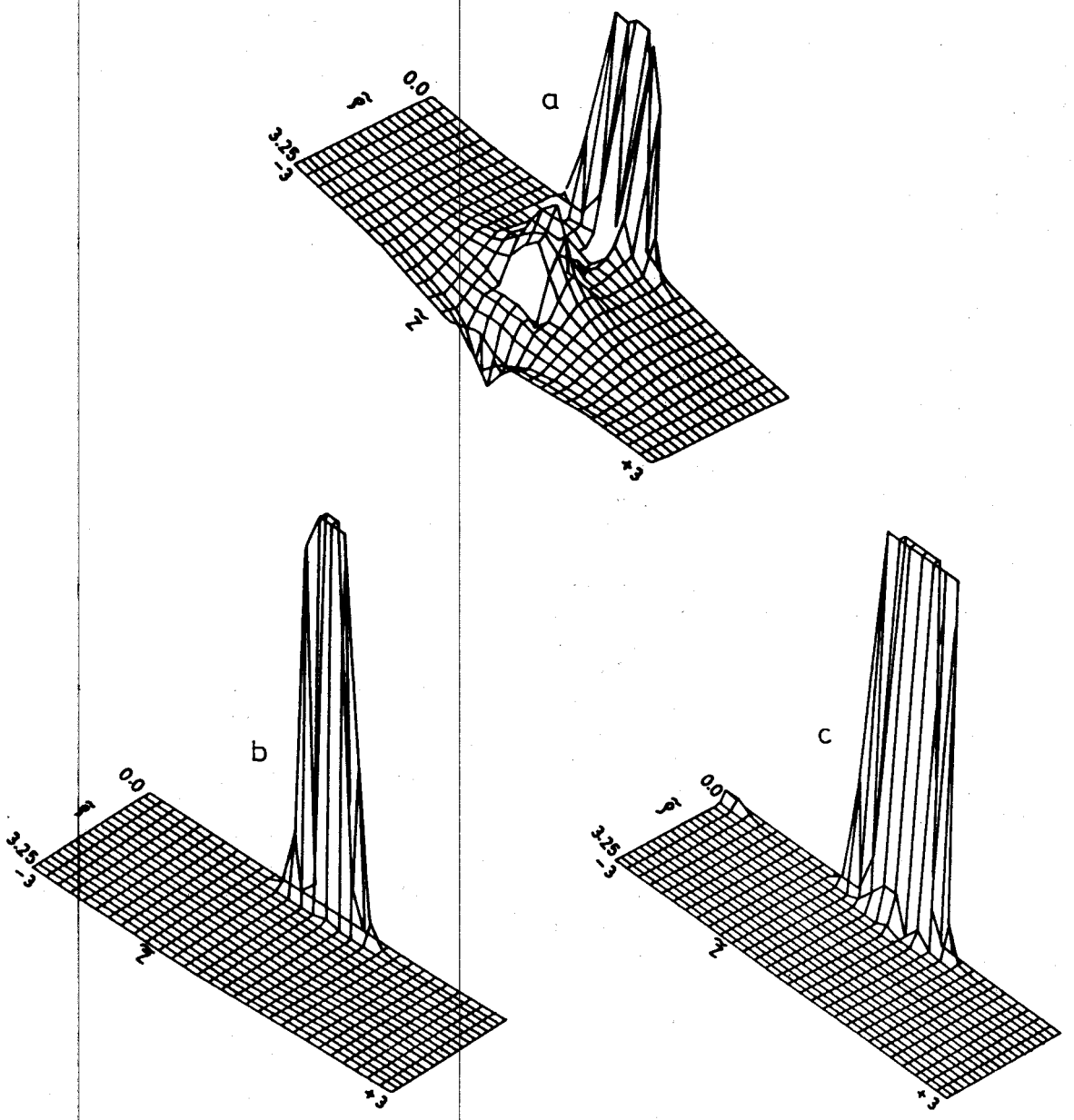

Fig. 2—Perspective plots (a.u.) of $\nu_{eff}(\mathbf{r}, t)$, $\rho(\mathbf{r}, t)$ and $|\mathbf{j}(\mathbf{r}, t)|$ for the proton-neon atom head-on collisions, in cylindrical polar coordinates. The basal rectangular mesh designates the $(\tilde{\rho}, \tilde{z})$ plane, where $0 \leq \tilde{\rho} \leq 3.25$ and $-3 \leq \tilde{z} \leq +3$. The target Ne nucleus is at (0, 0) and the proton is approaching from the left along the $\tilde{\rho} = 0$ direction of $\tilde{z}$. Here, $t = 0.08$, $R = 9.92$ a.u. (a) $-50 \leq \nu_{eff} \leq +50$, (b) $0 \leq \rho \leq 50$, (c) $0 \leq |\mathbf{j}| \leq 50$. (reproduced from ref. 20; courtesy, American Physical Society).

QFDFT of high-energy proton-helium collisions

In order to computationally follow the collision process from start to finish, we have developed a different GNLSE and a different, faster algorithm for 25 keV head-on collisions between a proton and a helium atom[21]. The basic equations are the same as Eqs (26)-(31), with the addition of a Wigner-Type local correlation functional,

$$E_C[\rho] = -\int \frac{\rho}{9.810 + 21.437\rho^{-1/3}}\, d\mathbf{r} \qquad \ldots(42)$$

and taking the KE functional as

$$T[\rho] = \frac{1}{8}\int \frac{|\nabla\rho|^2}{\rho}\, d\mathbf{r} \qquad \ldots(43)$$

The GNLSE, Eq. (36), retains its form, but $\nu_{eff}(\mathbf{r},t)$ now becomes,

$$\nu_{eff}(\mathbf{r}, t) = -\frac{4}{3}C_x\rho^{1/3} - \frac{7.146\rho^{-1/3}}{(9.810 + 21.437\rho^{-1/3})^2} - \frac{1}{9.810 + 21.437\rho^{-1/3}} - U(\mathbf{r}) - \frac{1}{|\mathbf{R} - \mathbf{r}|} \qquad \ldots(44)$$

As in the previous section, Eqs (36) and (44) are numerically solved in cylindrical polar coordinates for the p-He scattering system and the results are depicted in Figs 3 and 4. For the interacting system, the reorganization of the electron density as a result of collisions may be described in terms of the TD difference density (DD), defined as,

$$\Delta\rho(t)=\rho(t)-\rho(t=0.02) \quad \ldots(45a)$$

or,

$$\Delta\rho(R)=\rho(R)-\rho(R=9.98) \quad \ldots(45b)$$

This charge reorganization gives rise to the electronic part of the TD induced dipole moment, viz,

$$\langle D_{ind}^{(\tilde{z})}\rangle(t)=\int \tilde{z}\rho(r,t)dr \quad \ldots(46)$$

where $-\infty \leqslant \tilde{z} \leqslant +\infty$ is one of the cylindrical polar coordinates $(\tilde{\rho}, \tilde{z}, \tilde{\phi})$ for the scattering system and the electric field induced by the approaching proton is along the $\tilde{z}$ direction, i.e., the internuclear axis.

From Fig. 3, "the first thing to notice is the noncentrosymmetric nature of the He density. There is a depletion of electron density at and near the He nucleus and a buildup of density towards the approaching proton. The two peaks in the depletion region (negative $\Delta\rho$) of the interacting system gradually move up to the accumulation region (positive $\Delta\rho$). As the proton approaches the He nucleus and then recedes from it, the base of the deep negative well in $\Delta\rho$ widens and the well depth increases, signifying a continuing charge depletion from and near the He nucleus. As the proton moves closer to the He nucleus (R = 9.0 and 9.5 a.u.) from the left, an

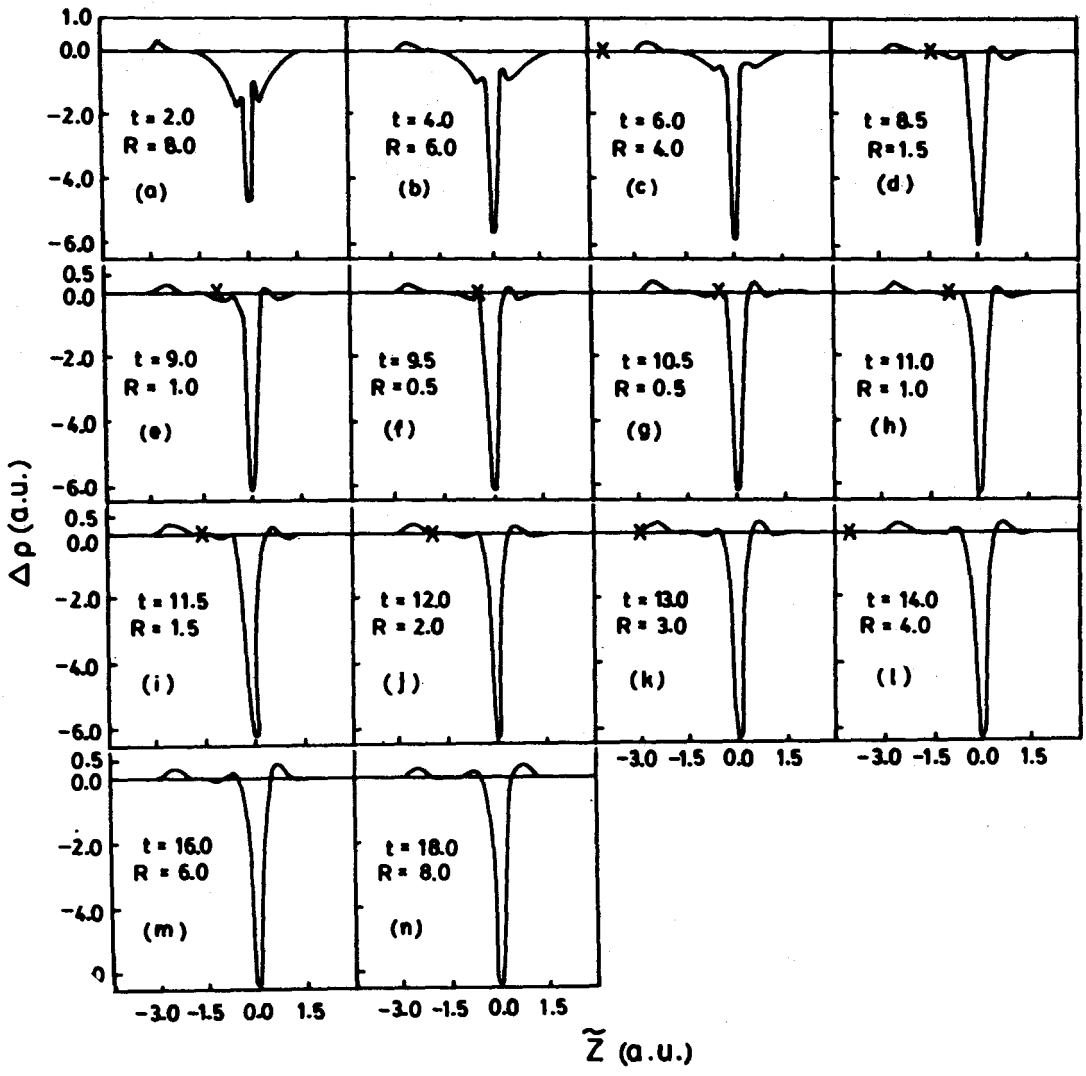

Fig. 3—Time-dependent difference density ($\Delta\rho$) profiles for the p-He scattering system along the $\tilde{z}$ axis for $\tilde{\rho}=0.0001$ (second mesh point in $\tilde{\rho}$) and $2 \leqslant t \leqslant 18$. The proton is approaching from the left and the He nucleus is at the origin. Except (a), (b), (m) and (n), the position of the proton is marked by a cross (×) on the $\tilde{z}$ axis (reproduced from ref. 21; courtesy, American Physical Society).

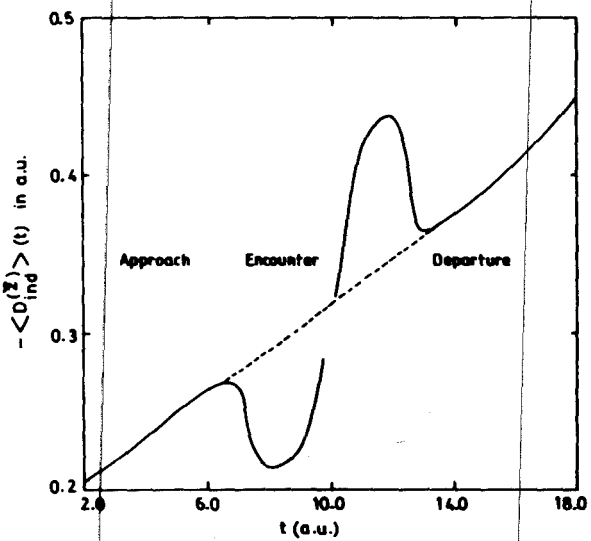

Fig. 4—Profile of the electronic part of the time-dependent induced-dipole moment, $-\langle D^{(\tilde{z})}_{ind}\rangle(t)$, for the *p*-He scattering system, for $2 \leqslant t \leqslant 18$. The dotted line shows an imaginary continuation of the *approach* regime into the *departure* regime, if there had been no *encounter* regime (reproduced from ref. 21; courtesy, American Physical Society).

electron density increase also occurs in the form of a peak to the right of the He nucleus. Initially, small fluctuations in the position and height of this peak can be observed. In the course of time, all three peaks with positive $\Delta\rho$ move to the right, even when the proton retraces its path to the original position. The distance between the two outermost peaks on both sides of the He nucleus remains practically the same throughout. At $t \simeq 7$, the proton enters the region of the charge buildup and, while returning, leaves this region at $t \simeq 13$. Thus causes the induced dipole moment to oscillate ... and enables us to partition the collision process into *approach* ($0 \leqslant t \leqslant 7$), *encounter* ($7 \leqslant t \leqslant 13$), and *departure* ($13 \leqslant t \leqslant 20$) regimes. From the nature of the $\Delta\rho$ profiles in Fig. 3, it is clear that into the original 1*s* density of the He atom, a substantial mixing of He pσ densities is taking place as a result of the interaction. The pronounced well in $\Delta\rho$ around the He nucleus indicates that the density is being largely replaced by excited-state densities with nodes at the He nucleus. Note that the present work does not consider a reactive collision leading to the formation of HeH^+. It is also clear that the present interaction leads to excitation but not ionization.

The TDDD profile at $t = 18.0$ is not the same as that at $t = 2.0$ although for both, $R = 8.0$. This indicates that even as the proton draws back from the He nucleus, along its original trajectory, the He electron density continues to respond to the proton. This is also true for $t = 20.0$. In order words, the He density does not have sufficient time to relax to its initial distribution" (quoted from ref. 21).

From Fig. 4, several interesting features have been observed. "First, the TD IDM shows distinct oscillations, with maxima at $t \simeq 7$ and 12, and minima at $t = 8.1$ and 13.1. As mentioned above, this naturally divides the interaction into approach, encounter, and departure regimes. Second, the TD IDM curve is nearly skew-symmetric about $t = 10.15$. Figure 4 clearly shows that if there had been no encounter regime between the proton and the He atom, the TD IDM curve at $t \simeq 7$ would have passed smoothly into the curve at $t \simeq 13$. Further, even though the receding proton is traversing its original line of approach, the TD IDM at $t = 18.0$ is not the same as that at $t = 2.0$, although both have the same R values. In other words, as already indicated by the $\Delta\rho$ profiles, a change of state of the system has taken place as a result of this interaction.

The negative sign of the TD IDM merely indicates that since the proton is approaching from the left (negative $\tilde{z}$), the He electron density begins to be polarized mainly to the left. A comparison of Figs 3 and 4 reveals that at $t \simeq 7$ the proton begins to penetrate the electron density buildup caused by itself and at $t \simeq 13$ the proton begins to leave the region of density buildup. From Fig. 3 it appears that the decrease in magnitude of the TD IDM after $t \simeq 7$ is due to the gradual emergence of a positive peak to the right of the He nucleus. And, at $t = 13.1$, the magnitude of the TD IDM begins to increase because of the appearance of a second positive $\Delta\rho$ peak to the left of the He nucleus. For $8 \leqslant t \leqslant 12$, the TD IDM increases in magnitude due to a continued accumulation of electron density to the left of the He nucleus. At $t \simeq 12$, the TD IDM magnitude decreases because of the continued density buildup to the right of the He nucleus and a movement of both the positive $\Delta\rho$ peaks to the right. Clearly, the TD IDM values reflect both the nature and the shifting of the electron density accumulation due to the TD interaction. Thus, the TD IDM shows pronounced nonlinear features in the encounter regime." (quoted from ref. 21).

Relation between the hydrodynamical phase and Berry's geometrical phase

Berry[10,26] has proved that solutions of the Schrödinger equation, corresponding to energy eigenstates, do not return to their original values but acquire a geometrical phase factor when transported slowly, i.e. adiabetically, around a closed loop in parameter space, where the parameters specify the systems's hamiltonian.

Sukumar and Deb[22] have further investigated the phase associated with the hydrodynamical "wave function" of a many-electron system, Eq. (28). It has been shown that this polar form leads to the appearance of an internal magnetic vector potential. A mathematical connection has been derived between the electronic phase and the Berry phase. This leads to a generalization of the current density concept and allows one to discuss the geometrical phase in terms of the circulation of this current in parameter space. For details, the reader may see ref. 22.

Conclusion

The amalgamation of two apparently independent approaches based on the single-particle density, *viz.* DFT and QFD, gives rise to TD GNLSEs which can describe the dynamics of TD processes such as proton-atom collisions. Such an approach is capable of revealing the non-linear features, if any, in the dynamics of the collision process. This is of considerable advantage in view of the fact that other quantum mechanical approaches to non-linear dynamics are still in their infancy. However, it is too early to speculate on the potential utility of the QFDFT approach reviewed in this article. A critical test of this approach could be to identify a TD process, with explicitly know non-linear features and then compare the calculated quantities, e.g., TDDD, TD induced dipole moment, etc., with the corresponding experimental results. It would also be necessary to deal with the very important phenomenon of *ionization* in proton-noble-gas-atom collisions. Only then one may conclude whether the conceptual appeal of QFDFT can be translated into new and penetrating physical insights into the mechanisms of TD processes such as atomic and molecular collisions.

Acknowledgement

We are thankful to the CSIR, New Delhi and Dept. of Atomic Energy, Bombay, for the financial support to our research projects on DFT and QFD. I am deeply indebted to my former students and colleagues, Dr Anjuli S Bamzai, Dr Swapan K Ghosh, Dr Pratim K Chattaraj, Dr N Sukumar and Ms Smitarani Mishra-Ota.

References

1 *The single-particle density in physics and chemistry*, edited by N H March & B M Deb (Academic Press, London), 1987.
2 Parr R G & Yang W, *Density-functional theory for atoms and molecules* (Oxford University Press, New York) 1989.
3 Kryachko E S & Ludena E V, *Energy density functional theory of many-electron systems* (Kluwer Academic Publishers, Dordrecht) 1990.
4 *Density functional theory of many-fermion systems* in Adv Quant Chem, edited by S B Trichey, Vol. 21 (Academic Press, New York) 1990.
5 Bamzai A S & Deb B M, *Rev Mod Phys*, 53 (1981) 95, 593.
6 Ghosh S K & Deb B M, *Phys Rep* 92 (1982) 1.
7 Deb B M & Ghosh S K, (ref. 1).
8 Horbatsch M & Dreizler R M, *Z Phys*, A 300 (1981) 119.
9 Horbatsch M & Dreizler R M, *Z Phys*, A 308 (1982) 329.
10 Berry M V, *Proc Roy Soc London*, A 392 (1984) 45.
11 Hohenberg P & Kohn W, *Phys Rev* 136 (1964) B864.
12 Parr R G, Donnelly R A, Levy M & Palke W E, *J chem Phys*, 68 (1978) 3801.
13 Kohn W & Sham L J, *Phys Rev*, 140 (1965) A1133.
14 Madelung E, *Z Phys*, 40 (1926) 332.
15 Hirschfelder J O, Goebel C J & Bruch L W, *J chem Phys*, 61 (1974) 5456.
16 Ghosh S K & Deb B M, *Int J Quant Chem*, 22 (1982) 871.
17 Deb B M & Ghosh S K, *J chem Phys*, 77 (1982) 342.
18 Gross E K U & Kohn W, (ref. 4).
19 Ghosh S K & Deb B M, *J Molec Struct Theochem*, 103 (1983) 163.
20 Deb B M & Chattaraj P K, *Phys Rev A*, 39 (1989) 1696.
21 Deb B M, Chattaraj P K & Mishra S, *Phys Rev*, A 43 (1991) 1248.
22 Sukumar N & Deb B M, *Int J Quant Chem*, 40 (1991) 501.
23 Ghosh S K & Balbas L, *J chem Phys*, 83 (1985) 5778.
24 *Chemical applications of atomic and molecular electrostatic potentials*, edited by P Potitzer & D G Truhlar (Plenum Press, New York), 1981.
25 Nelson E, *Dynamical theory of brownian motion* (Princeton University Press, Princeton) 1967.
26 Berry M V, *Phys Today*, December, 1990, p. 34.